frontiers in Earth Science

ORIGINAL RESEARCH
published: 23 February 2021
doi: 10.3389/feart.2021.625868

Observational Evidence of Distinguishable Weather Patterns for Three Types of Sudden Stratospheric Warming During Northern Winter

Hyesun Choi[1], *Joo-Hong Kim*[1], *Baek-Min Kim*[2]* *and Seong-Joong Kim*[1]*

[1]Division of Atmospheric Sciences, Korea Polar Research Institute, Incheon, Republic of Korea, [2]Department of Environmental Atmospheric Sciences, Pukyong National University, Pusan, Republic of Korea

Sudden stratospheric warming (SSW) events often lead to a cold surface air temperature anomaly over the extratropical regions. In this study, we propose, through observational evidence, that the types of SSW determine the severity of the cold anomaly. Based on the three-type classification of SSW, it is found that the surface air temperature drops notably over central to eastern North America following an SSW-type transition, especially from displacement to split. Note, however, that the differences in mean surface air temperature anomalies between SSW types are not statistically significant, even though after SSW-type transition from displacement to split, surface air temperature anomalies are colder than the other two types. The development of an anomalous tropospheric ridge in the North Pacific Arctic sector, associated with the difference in the vertical and zonal propagation of planetary waves, characterizes the post-warming period of the displacement–split type. After the occurrence of the displacement–split type transition of SSW events, upward propagation of planetary waves of zonal wavenumber 1 is suppressed, whereas planetary waves of zonal wavenumber 2 increase in the troposphere. Accompanying the ridge in the North Pacific, a trough developed downstream over North America that carries cold polar air therein. The results in this study are relevant for the subseasonal time scale, within 20 days after an SSW occurrence.

Keywords: sudden stratospheric warming, type-transition, North America, surface temperature, cold polar air

OPEN ACCESS

Edited by:
Chaim Garfinkel,
Hebrew University of Jerusalem, Israel

Reviewed by:
Ian White,
Hebrew University of Jerusalem, Israel
Daoyi Gong,
Beijing Normal University, China

***Correspondence:**
Baek-Min Kim
baekmin@pknu.ac.kr
Seong-Joong Kim
seongjkim@kopri.re.kr

Specialty section:
This article was submitted to Atmospheric Science, a section of the journal Frontiers in Earth Science

Received: *04 November 2020*
Accepted: *19 January 2021*
Published: *23 February 2021*

Citation:
Choi H, Kim J-H, Kim B-M and Kim S-J (2021) Observational Evidence of Distinguishable Weather Patterns for Three Types of Sudden Stratospheric Warming During Northern Winter. Front. Earth Sci. 9:625868. doi: 10.3389/feart.2021.625868

INTRODUCTION

There is increasing evidence that weak polar vortex states can account for cold winters over midlatitudes (Cellitti et al., 2006; Kolstad et al., 2010; Park et al., 2011; Kim et al., 2014; Kidston et al., 2015; Kretschmer et al., 2018a, Kretschmer et al., 2018b). However, not all polar vortex weakening events exhibit cold weather, and not all of them are accompanied by the same surface response (Nakagawa and Yamazaki, 2006; Mitchell et al., 2013; Lehtonen and Karpechko, 2016; Rao et al., 2020).

Extremely weak vortex states are often associated with Sudden stratospheric warmings (SSWs) characterized by rapid warmings in the polar stratosphere and a reversal of circumpolar westerlies. Using an objective algorithm based on the stratospheric polar vortex structure, Charlton and Polvani (2007) classified SSW events into two types: vortex displacement events and vortex splitting events. Whereas Charlton and Polvani (2007) concluded that the hemispheric influence of SSW on the

tropospheric state was not affected by the event type, Mitchell et al. (2013) identified different surface responses over North America and Eurasia between displacement and split events. They argued that the surface impact of split events was stronger than that of displacement events. Lehtonen and Karpechko (2016) also analyzed surface weather patterns related to major SSW events and classified them into displacement and split events based on reanalysis data and models. Through observational analysis, they showed that cold anomalies in northern Eurasia appeared before, rather than after, the SSW events, particularly for displacement events, even though the models failed to reproduce the cooling process. However, Maycock and Hitchcock (2015) and White et al. (2019) showed that the relative impact of the conventional two types could be subject to sampling issues due to the small number of SSW events.

SSW type can be classified based on the tropospheric response, wave mechanism, and SSW strength. Nakagawa and Yamazaki (2006) showed that downward propagating events tended to be accompanied by an enhanced upward flux of the wavenumber 2 during the prewarming period. Kodera et al. (2016) classified SSW events into absorbing and reflecting types based on the propagation property of planetary waves and revealed the different influences of SSW on the troposphere. Matthias and Kretschmer (2020) argued that cold spells over Europe and North America are related to different wave mechanisms, based on the analysis of two SSW events. Hitchcock et al. (2013), Maycock and Hitchcock (2015), and Karpechko et al. (2017) showed that lower-stratospheric anomaly during postwarming periods is crucial for assessing the surface impact by SSW. Rao et al. (2020) predicted the downward propagation and surface impact of two different types of SSW events in subseasonal to seasonal models and also revealed that the strength of the SSW is more critical than the vortex morphology and dominant wavenumber in determining the magnitude of its downward impact.

The difference in findings and discrepancies among the researchers renders it challenging to summarize the relationship between the SSW events and surface weather. Therefore, further research is required to understand the different results obtained using the other analysis methods and different target periods and generalize the relationship between weak vortex states and tropospheric cold events.

Choi et al. (2019) identified two distinct groups in conventional split-type SSW events using reanalysis data and objectively classified the conventional split type into displacement–split (DS) and split–split (SS) types. Based on the temporal evolution of the stratospheric polar vortex structure, the DS type in the conventional split type is characterized by the type of transition from the displacement type before the SSW to the split type after the SSW, and the remaining events are classified as the SS type, in which two vortexes are generally maintained both before and after the SSW. Therefore, the DS and SS types can be considered as transient and stationary split types, respectively. The conventional displacement type, characterized by a single displaced polar vortex both before and after SSW, is classified as a displacement–displacement (DD) type by applying the same naming system. Choi et al. (2019) found that the three SSW types display different characteristics in upward-propagating wave activity and a tropospheric height field during the pre-warming period. They showed that the results based on the traditional two-type classification (Charlton and Polvani, 2007) could weaken the distinct features between DS and SS types, and suggested that DS-type SSW events should be objectively defined to improve the understanding of SSW-related phenomena. In their extended study, differences in tropospheric precursor patterns over the North Atlantic between DD- and DS-type SSW were identified (Choi et al., 2020).

Following the studies conducted by Choi et al. (2019); Choi et al. (2020), we investigate the surface responses over midlatitudes based on the three-type classification of SSW (Choi et al., 2019). The current study will provide observational evidence on how the regional wintertime climate varies depending on the SSW type. In addition, because the dependence of the cold events in midlatitudes on the type of SSW can help in the prediction of the tropospheric weather (Kodera et al., 2008; Mitchell et al., 2013; Matthias and Kretschmer, 2020), information on SSW events based on the different types of SSW can be useful for predicting the occurrence of cold weather in midlatitudes, especially North America, on the subseasonal time scale. The data and methods adopted in the current study are described in *Data and Methods section* and the results are described in *Results* section. The summary is presented in *Summary* section.

DATA AND METHODS

We use the reanalysis dataset from the National Centers for Environmental Prediction–National Center for Atmospheric Research (NCEP–NCAR) developed over January 1, 1957 to December 31, 2014 (Kalnay et al., 1996). This dataset has a horizontal resolution of 2.5° latitude × 2.5° longitude at 17 pressure levels from 1,000 to 10 hPa. The daily climatological values of each atmospheric variable are calculated based on the period 1981–2010, and are smoothed by a 31-day running mean. Anomaly fields are defined by deviations from these climatological means. In this study, we determine statistical significance from a zero at the 90% confidence level based on Student's two-sided *t*-test.

Major SSW events are detected by wind reversal at 10 hPa and 60°N. The first day of wind reversal is defined as the central day (Day 0). Major SSW events and their types for the period 1957–2014 are chosen, according to Table 1 in Choi et al. (2019). During the analysis period, the numbers of DD-, DS-, and SS-type events occurred 20, 10, and 7 times, respectively. These events are used for composite analysis.

RESULTS

Figure 1 presents the composite mean of 1,000 hPa temperature anomalies (shading) and 300 hPa geopotential height (GPH) anomalies (contours) before (days -20 to -5) and after (days 5

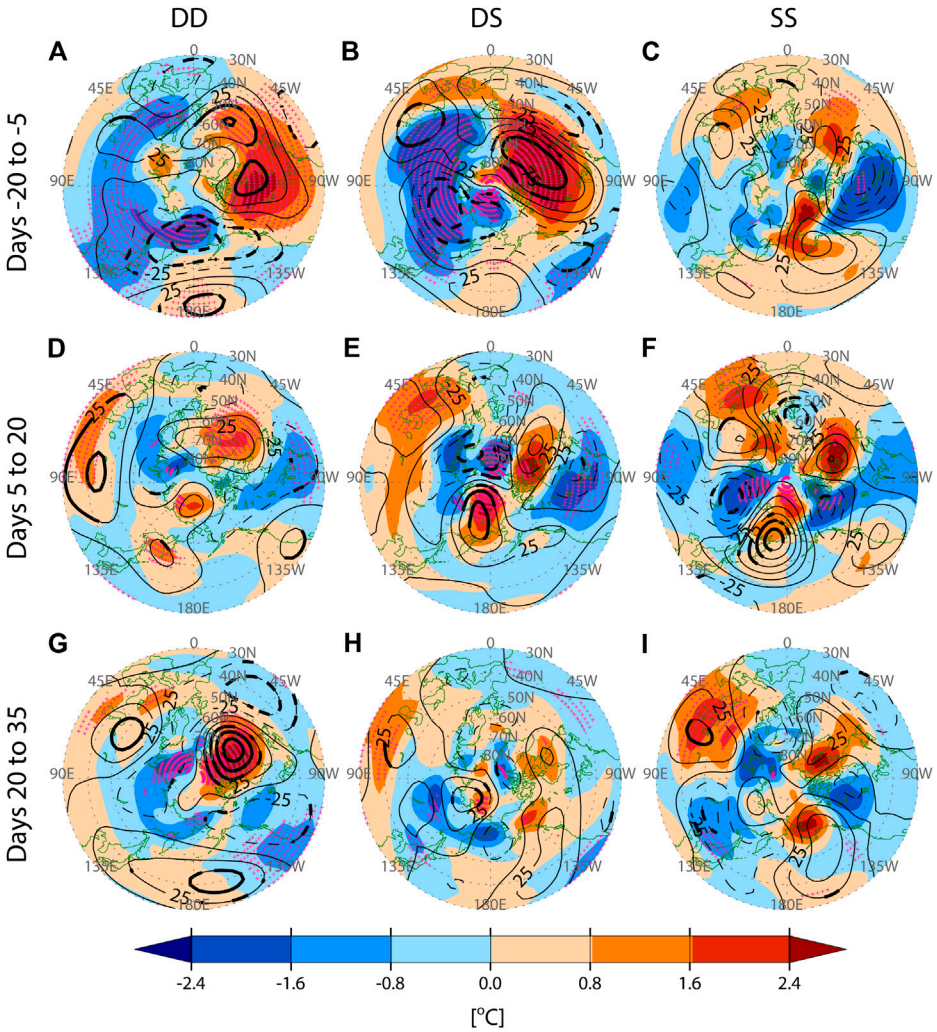

FIGURE 1 | Temperature anomaly at 1,000 hPa **(shading)** and geopotential height (GPH) anomaly at 300 hPa (contours) for zonal wave components from 1 to 5. The results are shown for **(A,D,G)** Displacement–displacement (DD); **(B,E,H)** Displacement–split (DS); and **(C,F,I)** Split–split (SS) sudden stratospheric warming (SSW) events, averaged **(Top)** from days -20 to -5, **(middle)** from days 5 to 20, and **(bottom)** from days 20 to 35. Contour interval is 25 m. Sold and dashed contours denote positive and negative values, respectively. Pink dots and bold contours indicate significant regions at 90% confidence level in temperature anomaly and GPH anomaly, respectively.

to 20 and days 20 to 35) the central day according to SSW types. Before SSW, in DD (**Figure 1A**) and DS (**Figure 1B**) types, positive GPH anomaly over the North Atlantic and negative GPH anomaly over the North Pacific are prominent, although the location of the trough centers near the North Pacific differs. The Atlantic ridge and Pacific trough correlate with vortex weakening by constructive interference with climatological wave-1 height field (Garfinkel et al., 2010). For both types, cold anomaly over Eurasia and warm anomaly over North America are identified. According to Kolstad et al. (2010), a precursor signal of warming aloft in the form of wave-1 GPH anomaly is associated with long-lived and robust cold anomalies over Asia and Europe. While the DS type shows atmospheric circulation patterns similar to the DD type before the central day, in SS type (**Figure 1C**), a positive GPH anomaly is identified over the northeast North Pacific. The ridge over the northeast North Pacific, although not significant here, is favorable for wave-2 development and one of the characteristic features of SS type (Choi et al., 2019). The cold anomaly and overlying trough are shown in North America.

Numerous studies have shown that ridge in the Pacific and the downstream trough over North America provide favorable conditions for the northerly flow between these two centers that results in low surface temperature over North America, and have suggested the causes inducing this overlying circulation pattern, as a tropical influence or Arctic warming (Carrera et al., 2004; Hartmann, 2015; Kug et al., 2015; Sung et al., 2016, 2019). Carrera et al. (2004) examined the composite structure and temporal evolution of Alaskan blocking events, which is a persistent atmospheric anticyclonic ridge over the northeast Pacific. They showed that the mature block was associated with pronounced troughing downstream over North America, using reanalysis data. The anomalous cyclonic flow in

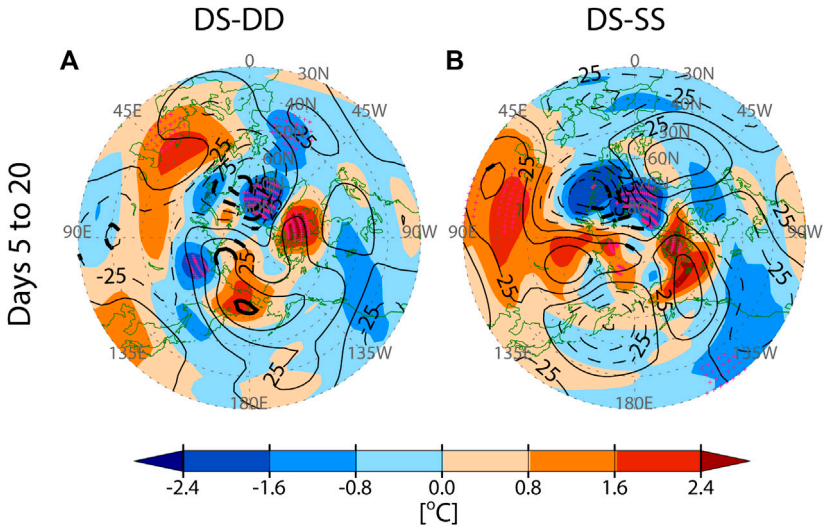

FIGURE 2 | Differences in temperature anomaly at 1,000 hPa and geopotential height (GPH) anomaly at 300 hPa averaged from days 5 to 20 **(A)** between DS and DD types, and **(B)** between DS and SS types. Pink dots and bold contours indicate significant regions at 90% confidence level in temperature difference and GPH difference, respectively.

the downstream regions can be explained by Rossby wave propagation from the upstream North Pacific ridge anomaly. Although blocking is not analyzed in this study, North Pacific high anomaly can be related to more frequent North Pacific blocking events (Renwick and Wallace, 1996).

During the first postwarming period (days 5 to 20), the cold anomaly over Eurasia diminishes in magnitude for both DD and DS types (**Figures 1D,E**). Simultaneously, the cold anomaly appears over North America by the strengthening of the North Pacific ridge. The ridge in the North Pacific and the trough in North America are consistent with the atmospheric circulation pattern in favor of the North American cold weather discussed above. In particular, the overlying atmospheric circulation after DS type (**Figure 1E**) appears similar to that before SS type (**Figure 1C**), and substantial cold anomalies are identified in central North America (120–80°W, 40–55°N). This provides observational evidence for the outbreak of cold waves in central North America within the conventional split type. For SS type (**Figure 1F**), as the wave-3 pattern develops, a downstream trough and a significant cold anomaly are limited to northwestern North America, despite the strong ridge of the Northwest Pacific.

During the second postwarming period (days 20 to 35), the North Pacific ridge in all types weakens, and the amplitude of the cold anomaly in North America also decreases. For the DD type (**Figure 1G**), positive GPH anomaly in the northern North Atlantic and negative GPH anomaly in the southern North Atlantic occur. The negative North Atlantic Oscillation (NAO)-like pattern is often associated with the weakening of the polar vortex (Baldwin and Dunkerton, 2001). However, for DS and SS types (**Figures 1H,I**), the North Atlantic response is relatively uncertain. According to Choi et al. (2020), for DS type, the negative NAO phase can be considered a precursor rather than a response. Afargan-Gerstman and Domeisen (2020) found that the anomalous weather patterns in the Pacific may contribute to the sign of the Atlantic response by synoptic storm propagation from the East Pacific toward the Atlantic. **Figures 1G–I** show the possibility that, during the second postwarming period, North Atlantic responses are different depending on SSW types.

Figure 1 shows temporally and geographically distinct cold anomalies and pressure anomalies through the life cycle of SSW events according to SSW types and provides the composite results for cold wave over North America, especially for DS type, that have not been examined in detail before.

We note the drop in near-surface temperature anomaly over central to eastern North America for DS type during days 5 to 20 (**Figure 1E**) and perform a significance test for the differences in near-surface temperature anomalies and tropospheric GPH anomalies between SSW types. **Figure 2** shows that after the DS-type SSW events, the near-surface temperature anomalies are colder than the other two types. However, the differences in surface temperature anomalies over central North America are not statistically significant. **Figure 2B** also shows that in northwestern North America, where a strong cold anomaly is identified for SS type (**Figure 1F**), the difference in the near-surface temperature between DS and SS is not statistically significant even though the near-surface temperature anomaly for DS type is relatively warmer. In **Figure 2A**, the positive GPH anomaly differences over the northern part of the North Pacific region (north of 60°N) indicate that the development of the ridge in the region for the DS type is pronounced compared to DD type. On the other hand, in **Figure 2B**, the difference in GPH anomaly between the DS and SS types in the region is uncertain. For both cases, the near-surface temperature anomaly over Scandinavia and Northern Europe (40°W-40°E, 60°N-75°N) are colder for the DS type than the other two types. The significant negative difference in GPH anomaly in these regions between DS and the other two types in **Figure 2** is related to the deepening of the trough for DS type (**Figure 1E**).

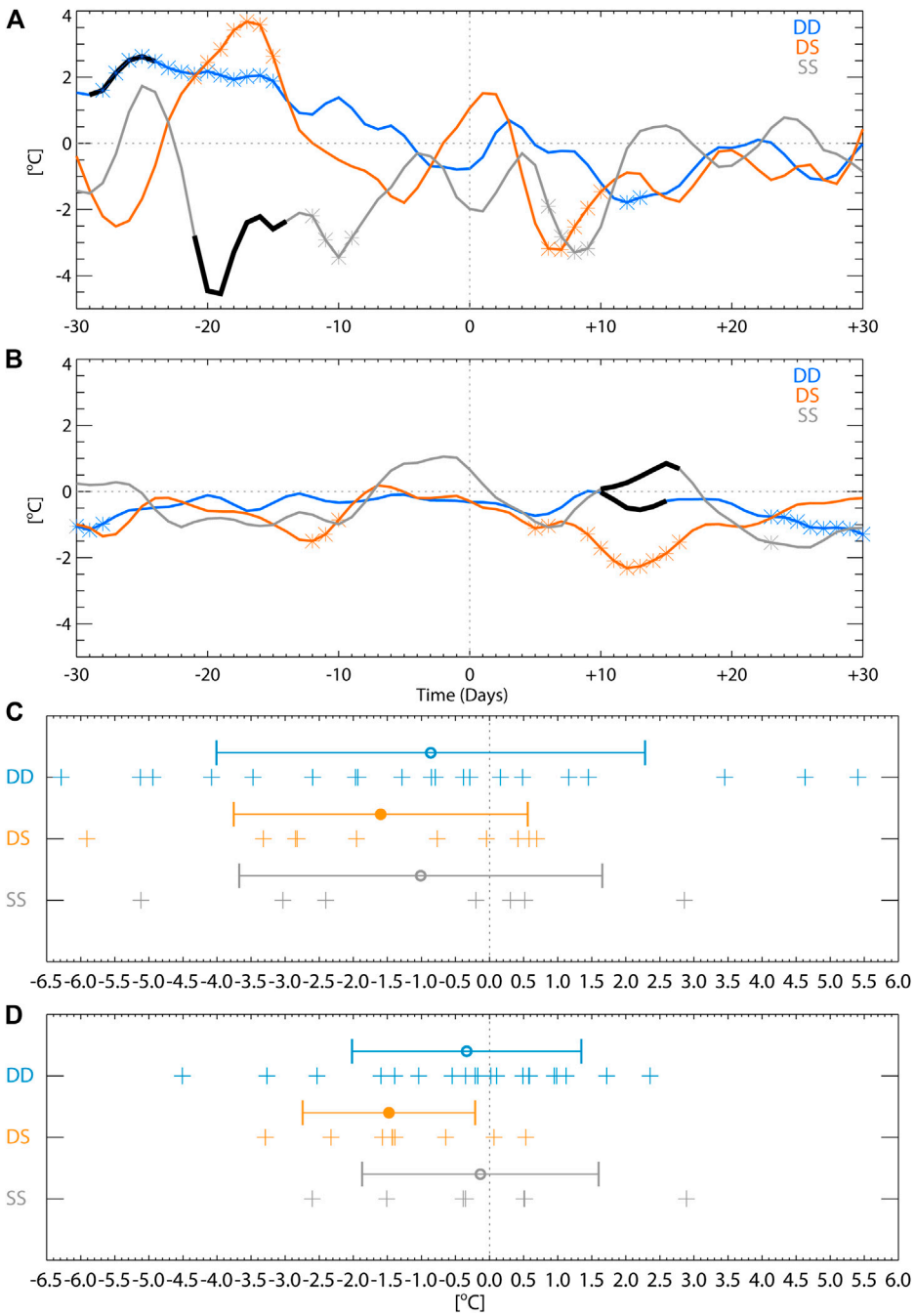

FIGURE 3 | (A) Time series of the 3-day running mean temperature anomaly at 1,000 hPa averaged over **(A)** North American (80°–120°W, 40°N–55°N) and **(B)** Scandinavia/Northern Europe (40°W-40°E, 60°N-75°N). Blue, orange, and gray lines denote DD, DS, and SS SSW types, respectively. The asterisk indicates statistically significant periods from a zero at 90% confidence level. The black bold solid part indicates when the DS minus DD and DS minus SS differences are significantly different at 90% confidence level, respectively. Scatter plot of temperature anomaly at 1,000 hPa over **(C)** North America and **(D)** Scandinavia/Northern Europe occurring during the three SSW types. The temperature anomaly is averaged over days 5 to 20. The mean temperature anomaly for each type is denoted by a closed circle with an error bar, indicating one standard deviation. The filled circle represents a statistically significant value at a 90% confidence level.

To investigate the temporal evolution of the surface temperature over North America according to the SSW type in more detail, a time series temperature index averaged over central North America is depicted in **Figure 3A**. As shown in **Figure 1**, the warm anomalies during the prewarming period change into cold anomalies after the occurrence of the event for the DD and DS types. In contrast, for the SS type, the cold anomaly develops before the central day and gradually weakens

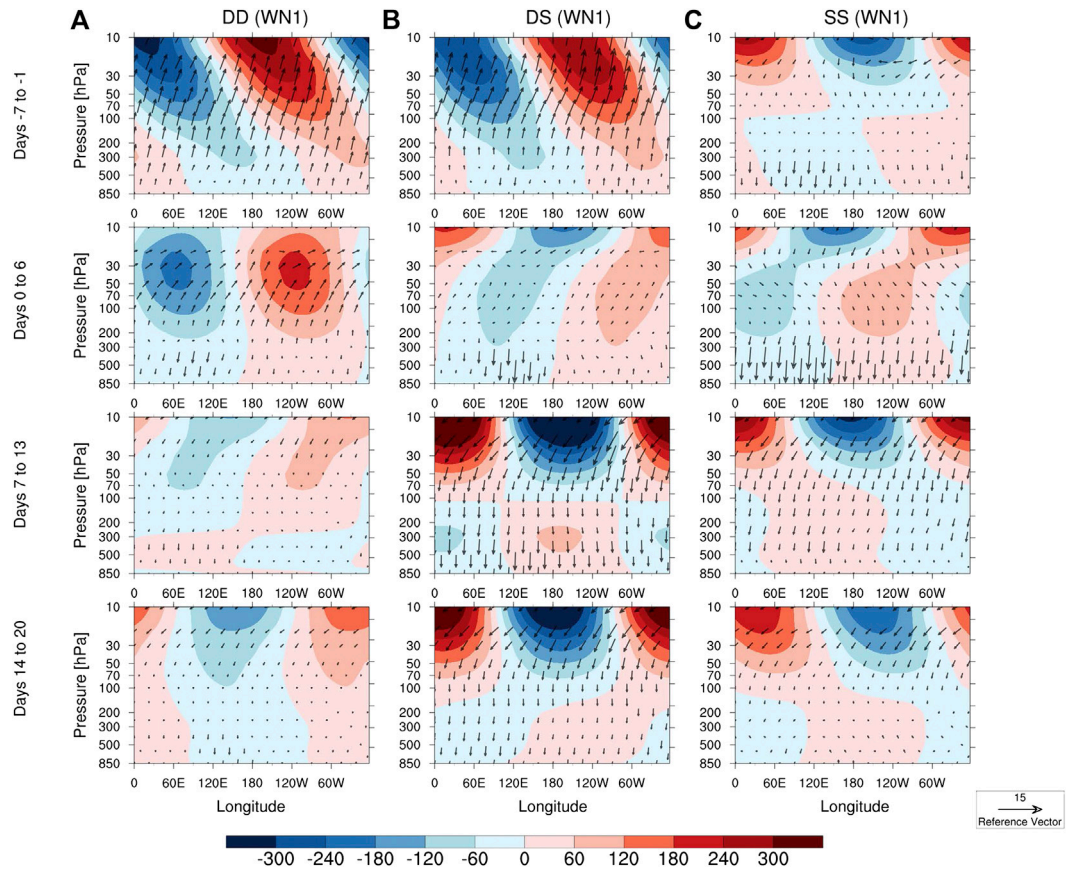

FIGURE 4 | (Continued).

over time. The difference in the timing of development of the North pacific ridge and the North America trough (**Figures 1C,E**) can be related to the difference in the temporal evolution of near-surface temperature over North America between DS and SS types. Using the traditional two-type classification (Charlton and Polvani, 2007), where the DS and SS types are not distinguished, identifying the difference in this type of temperature trend is challenging. The temperature difference between the DS and SS types is robust during the prewarming period rather than during postwarming period, especially between days -21 to -14. During this period, near-surface temperature over North America for SS type is significantly colder than for DS type. The near-surface temperature transition from the maximum (day -17) to the minimum (day 7) peaks is more rapid in the DS-type period than the DD-type period. The temperature over North America is further examined based on the temperature index averaged over days 5–20 (**Figure 3C**). A total of 7 cold anomalies are observed out of 10 DS-type events, 13 out of 20 DD-type events, and 4 out of 7 SS-type events. Considering the mean value of the temperature anomaly, the DD- and SS-type results are statistically insignificant, and only the cold event from the DS-type result is statistically significant. The robust cold anomaly over North America for DS type indicates that the near-surface cold anomaly is less varying than other SSW types and could occur more frequently after the events. Therefore, not only the mean difference between SSW types but also the significance of the mean value itself can provide useful information regarding predictability. **Figures 3B,D** show temperature evolution and index for Scandinavia and Northern Europe, where the cold anomaly is more prominent after the DS-type SSW events but is weaker or uncertain after other types. The temperature difference between the DS type and the other two types is significantly lower for about a week after day 10 at the 90% significant level. In **Figure 3D**, a total of 8 cold anomalies are observed out of 10 DS-type events, 10 out of 20 DD-type events, and 4 out of 7 SS-type events. Considering the mean value of the temperature anomaly, only the cold event from the DS-type result is statistically significant.

To investigate the origin of the ridge over the North Pacific Arctic sector, we calculate the planetary-scale wave activity associated with the North Pacific circulation exhibiting a three-dimensional (3-D) wave activity flux (Takaya and Nakamura, 2001). The longitude-height sections of the 3-D wave activity flux anomaly averaged over 50–60°N for the zonal-wave component waves 1 and 2, together with GPH anomaly averaged over 60–70°N, are depicted in **Figure 4**. The GPH anomaly is also shown in **Figure 4** for the zonal-wave 1 and 2 components, respectively. We display from day -7 to day 20,

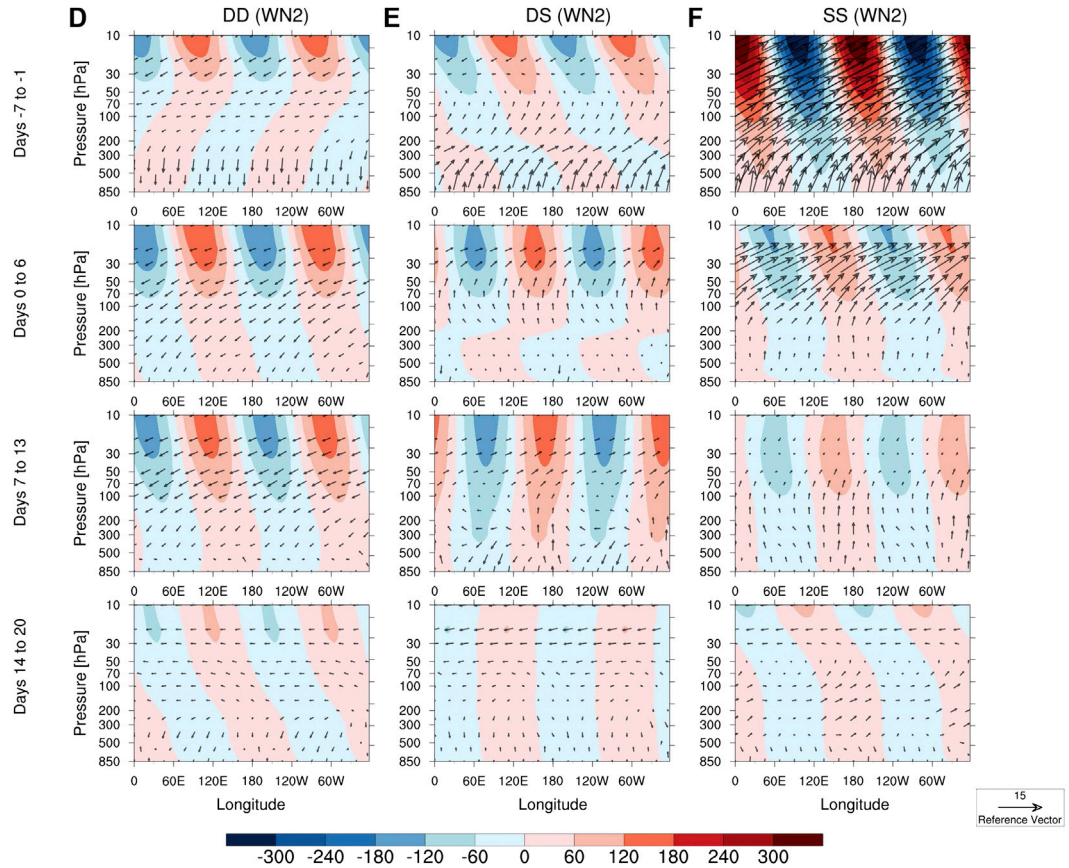

FIGURE 4 | (A)–(C) Longitude-height sections of geopotential height anomaly (shading) averaged over 60°N–70°N, and zonal and vertical components of the 3-D wave activity flux anomaly (arrows) averaged over 50°N–60°N, calculated from wave 1 component. From the top to bottom, each panel shows the results averaged over 7 days from days -7 to 20. The color interval is 100 m. Arrows at the bottom right indicate the magnitude of the zonal and vertical components of 3-D wave activity flux [m^2 s^{-2}]. The 3-D wave activity flux is scaled by $\sqrt{\frac{1000}{p}}$ for the zonal component and by $150 \times \sqrt{\frac{1000}{p}}$ for the vertical component. The p is the pressure at each level. **(A)** DD; **(B)** DS; and **(C)** SS SSW types. **(D)–(F)** As in **(A)–(C)** but for wave 2 component.

because the circulation pattern associated with wave activity remained almost the same before day -7 and after day 20.

As shown in Choi et al. (2019), before the central day (days -7 to -1), wave-1 GPH anomalies are predominant in DD and DS types (**Figures 4A,B**), and their ridges and troughs shift westward toward the upper level and are in phase with winter climatological wave-1 pattern (See **Supplementary Figure S1A**), which indicates a favorable structure for upward propagation of the planetary wave (Charney and Drazin, 1961). The upper-level tropospheric ridge is located over the Atlantic sector. The wave-1 field for the SS type shows negligible amplitude (**Figure 4C**), but the wave-2 field (**Figure 4F**) is developed in phase with the climatological wave (See **Supplementary Figure S1B**) and propagates upward from the troposphere to the stratosphere (**Figure 4F**). For wave-1 component, temporal changes in the zonal and vertical structure of GPH anomaly and upward propagation properties of the wave before and after the central day appear to be much more dramatic for the DS type than other types. During days 7-13, for the DS type, the ridge and trough lines with height are out of phase with the winter climatological wave-1 pattern, and anomalous downward propagation is prominent. At the same time, a tropospheric ridge develops near 180°E. During days 14-20, for the DS type, the anomalous downward propagation and the North Pacific ridge slightly weaken.

Choi et al. (2019) showed that the role of the wave-2 component was marginal throughout the period in the DD type, whereas in DS type, it began to increase a few days before the central day. As in the previous finding, **Figure 4D** also shows that during days -7 to -1, for DD type, wave-2 field propagates downward to the lower level, whereas for DS type (**Figure 4E**), upward propagation from the troposphere to the upper level is identified. The upward propagation of wave 2 for DS type is temporarily weakened in the troposphere just after the central day (days 0-6) but reinforces during days 7 to 13. Between two periods (days -7 to -1 and days 7 to 13), the upper-tropospheric ridge development in the North Pacific region for DS type seems to be more pronounced than for other types. After SS type (**Figure 3F**), the wave-2 field somewhat weakens. Considering only extreme-long waves (waves 1 and 2), the tropospheric North Pacific ridge development after SS type is not as evident (**Figure 1F**). This means that the North Pacific

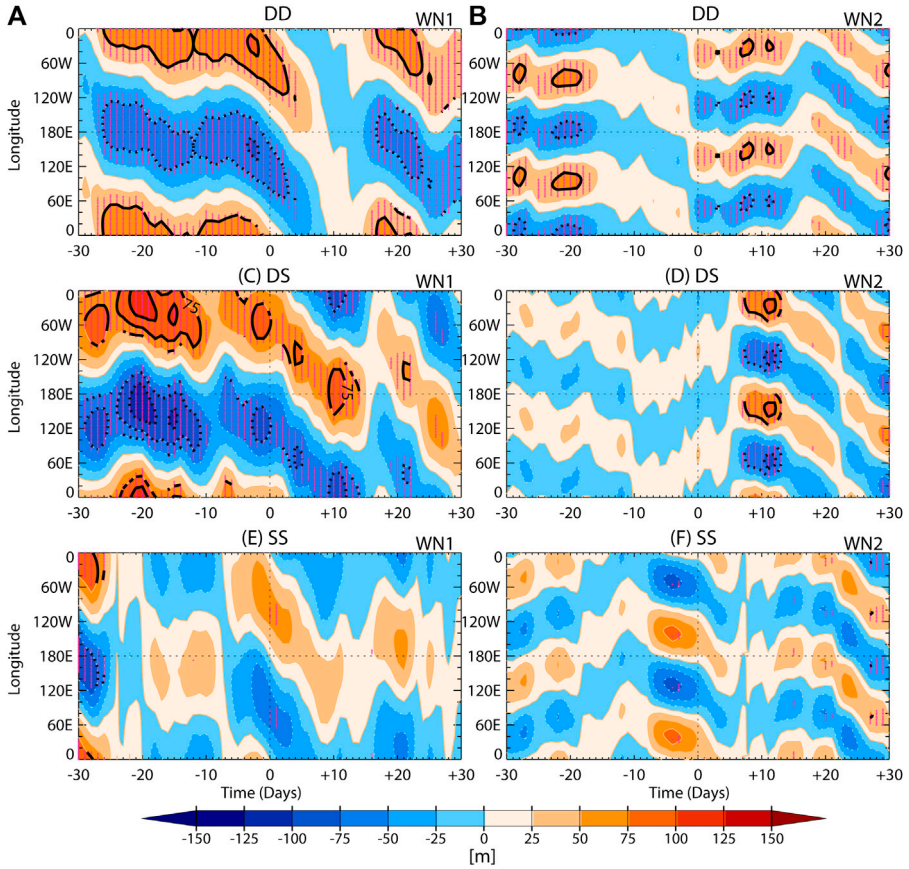

FIGURE 5 | Time-longitude sections of the anomalous geopotential height **(A,C,E)** wave 1, and **(B,D,F)** wave 2 averaged over 60°N–70°N at 300 hPa for **(Top)** DD, **(Middle)** DS, and **(Bottom)** SS SSW types. The color interval is 25 m. Bold contours and pink dots indicate significant regions at 90% confidence level.

ridge development after SS type is associated with wave activity with wave 3 or higher.

Choi et al. (2019) showed that the stratospheric polar vortex split into a wave 2 pattern around day 5 after the central day during DS-type SSW. **Figures 4B,E** show the weakening of wave 1 activity, increase of wave 2 activity, and the North Pacific ridge development in the troposphere during days 7–13 for the DS type, all of which are identified following the occurrence of type transition from the displacement to split in the stratosphere.

To show the detailed structural changes of the tropospheric GPH anomaly in **Figure 4**, the time-longitude sections of the wave 1 and 2 GPH anomalies are depicted in **Figure 5**, respectively. For the DD and DS types (**Figures 5A,C**), before the central day, the position of the North Pacific ridge (60°E–60°W) and trough (120°W–120°E) of wave 1 GPH anomaly is almost stationary, but after the central day, the wave 1 GPH anomaly propagates westward. For the DD type (**Figure 5A**), its amplitude diminishes rapidly for approximately two weeks after the central day. The trough in the North Pacific sector and the ridge in the North Atlantic sector reappear. In contrast, for the DS type (**Figure 5C**), its amplitude persists even after the SSW event and around day 10, an amplification of the positive anomaly appears at approximately 180°E. This period coincides with the time during which there is an anomalous downward propagation of the wave 1 component (**Figure 4B**). The anomalous North Pacific ridge temporarily weakens but develops again around day 20. The development of the wave 2 anomaly after the central day (**Figure 5D**) is also prominent around day 10. The high-pressure anomaly at approximately 180°E in the North Pacific and a low-pressure anomaly at 60–120°W, corresponding to North America, is consistent with the circulation pattern associated with the significant cold anomaly in North America, as identified in **Figure 1E**. As discussed in **Figure 4**, it is difficult for the SS type to show the original observed features by considering only waves 1 and 2. The wave 1 evolution after the central day (**Figure 5E**) seem to be similar to the DS type (**Figure 5C**) but smaller in amplitude. Although it is re-amplified after day 20, it is not significant. The large wave 2 amplitude before the central day (**Figure 5F**) substantially decreases after the central day.

SUMMARY

In this study, observational evidence for features in weather patterns based on the three types of SSW events is provided

through a composite analysis using reanalysis data. The surface temperature over North America becomes rapidly cold after the occurrence of DS-type SSW events. This is probably due to the high-pressure anomaly that continuously appears and strengthens around the North Pacific, leading to the formation of a downstream trough and cold weather.

The development of a North Pacific ridge in the troposphere is associated with the difference in the vertical and zonal propagation of planetary waves and the vertical structure of planetary waves. The temporal evolution of the wave 1 GPH anomaly shows that, during the DS-type period, the high-pressure anomaly in 0–120°W before SSW propagates westward after SSW and the subsequent high-pressure anomaly near 180°E and low-pressure anomaly over 60–120°W emerge. These circulation patterns are associated with cold weather in North America.

Although this study mainly describes winter weather in North America, the large cold anomaly over Scandinavia and Northern Europe after DS-type SSW events (**Figure 1E**) is also noteworthy. The cold anomaly in this region is prominent after the DS-type SSW events but is weaker or uncertain after other types. The temperature difference between the DS type and the other two types is significantly lower for about a week after day 10 at the 90% significant level.

We focus mainly on the observational dependence of the tropospheric response on the different SSW types, leaving the question of a causal relationship between planetary-wave development and wave-propagation properties after the DS-type SSW for a future study.

The results suggest that DS-type SSW information could be utilized to improve forecasts of cold weather over North America, although the mechanism for the development of the North Pacific ridge remains to be investigated.

DATA AVAILABILITY STATEMENT

Publicly available datasets were analyzed in this study. This data can be found here: https://psl.noaa.gov/data/gridded/data.ncep.reanalysis.pressure.html.

AUTHOR CONTRIBUTIONS

HC, BK, and SK initiated and coordinated the work. HC provided the calculation. HC wrote the manuscript, and SK, BK, and JK revised it. SK, BK, and JK gave valuable suggestions for analysis.

FUNDING

This study was funded by the project "Earth System Model-based Korea Polar Prediction System (KPOPS-Earth) Development and Its Application to the High-impact Weather Events originated from the Changing Arctic Ocean and Sea Ice" (KOPRI, PE21010). B-MK is supported by the project entitled "Korea-Arctic Ocean Observing System (K-AOOS), KOPRI, 20160245," funded by the MOF, Korea.

SUPPLEMENTARY MATERIAL

The Supplementary Material for this article can be found online at: https://www.frontiersin.org/articles/10.3389/feart.2021.625868/full#supplementary-material.

REFERENCES

Afargan-Gerstman, H., and Domeisen, D. I. V. (2020). Pacific modulation of the North Atlantic storm track response to sudden stratospheric warming events. *Geophys. Res. Lett.* 47, e2019GL085007. doi:10.1029/2019GL085007

Baldwin, M. P., and Dunkerton, T. J. (2001). Stratospheric harbingers of anomalous weather regimes. *Science* 294, 581–584. doi:10.1126/science.1063315

Carrera, M. L., Higgins, R. W., and Kousky, V. E. (2004). Downstream weather impacts associated with atmospheric blocking over the Northeast Pacific. *J. Clim.* 17, 4823–4839. doi:10.1175/jcli-3237.1

Cellitti, M. P., Walsh, J. E., Rauber, R. M., and Portis, D. H. (2006). Extreme cold air outbreaks over the United States, the polar vortex, and the large-scale circulation. *J. Geophys. Res.* 111, D02114. doi:10.1029/2005jd006273

Charlton, A. J., and Polvani, L. M. (2007). A new look at stratospheric sudden warmings. Part I: climatology and modeling benchmarks. *J. Clim.* 20, 449–469. doi:10.1175/jcli3996.1

Charney, J. G., and Drazin, P. G. (1961). Propagation of planetary-scale disturbances from the lower into the upper atmosphere. *J. Geophys. Res.* 66, 83–109. doi:10.1029/jz066i001p00083

Choi, H., Choi, W., Kim, S. J., and Kim, B. M. (2020). Dependence of sudden stratospheric warming type-transition on preceding North Atlantic oscillation conditions. *Atmos. Sci. Lett.* 21 (3), e953. doi:10.1002/asl.953

Choi, H., Kim, B.-M., and Choi, W. (2019). Type classification of sudden stratospheric warming based on pre- and postwarming periods. *J. Clim.* 32, 2349–2367. doi:10.1175/jcli-d-18-0223.1

Garfinkel, C. I., Hartmann, D. L., and Sassi, F. (2010). Tropospheric precursors of anomalous Northern hemisphere stratospheric polar vortices. *J. Clim.* 23, 3282–3299. doi:10.1175/2010jcli3010.1

Hartmann, D. L. (2015). Pacific sea surface temperature and the winter of 2014. *Geophys. Res. Lett.* 42, 1894–1902. doi:10.1002/2015gl063083

Hitchcock, P., Shepherd, T. G., and Manney, G. L. (2013). Statistical characterization of Arctic polar-night jet oscillation events. *J. Clim.* 26, 2096–2116. doi:10.1175/jcli-d-12-00202.1

Kalnay, E., Kanamitsu, M., Kistler, R., Collins, W., Deaven, D., Gandin, L., et al. (1996). The NCEP/NCAR 40-year reanalysis project. *Bull. Am. Meteorol. Soc.* 77, 437–471. doi:10.1175/1520-0477(1996)077<0437:tnyrp>2.0.co;2

Karpechko, A. Y., Hitchcock, P., Peters, D. H. W., and Schneidereit, A. (2017). Predictability of downward propagation of major sudden stratospheric warmings. *Q. J. R. Meteorol. Soc.* 104 (30), 937. doi:10.1002/qj.3017

Kidston, J., Scaife, A. A., Hardiman, S. C., Mitchell, D. M., Butchart, N., Baldwin, M. P., et al. (2015). Stratospheric influence on tropospheric jet streams, storm tracks and surface weather. *Nat. Geosci.* 8, 433–440. doi:10.1038/ngeo2424

Kim, B. M., Son, S. W., Min, S. K., Jeong, J. H., Kim, S. J., Zhang, X., et al. (2014). Weakening of the stratospheric polar vortex by Arctic sea-ice loss. *Nat. Commun.* 5, 4646. doi:10.1038/ncomms5646

Kodera, K., Mukougawa, H., and Itoh, S. (2008). Tropospheric impact of reflected planetary waves from the stratosphere. *Geophys. Res. Lett.* 35, L16806. doi:10.1029/2008gl034575

Kodera, K., Mukougawa, H., Maury, P., Ueda, M., and Claud, C. (2016). Absorbing and reflecting sudden stratospheric warming events and their relationship with tropospheric circulation. *J. Geophys. Res. Atmos.* 121, 80–94. doi:10.1002/2015jd023359

Kolstad, E. W., Breiteig, T., and Scaife, A. A. (2010). The association between stratospheric weak polar vortex events and cold air outbreaks in the Northern hemisphere. *Q. J. R. Meteorol. Soc.* 136, 886–893. doi:10.1002/qj.620

Kretschmer, M., Cohen, J., Matthias, V., Runge, J., and Coumou, D. (2018b). The different stratospheric influence on cold-extremes in Eurasia and North America. *npj Clim. Atmos. Sci.* 1, 44. doi:10.1038/s41612-018-0054-4

Kretschmer, M., Coumou, D., Agel, L., Barlow, M., Tziperman, E., and Cohen, J. (2018a). More-persistent weak stratospheric polar vortex states linked to cold extremes. *Bull. Am. Meteorol. Soc.* 99, 49–60. doi:10.1175/bams-d-16-0259.1

Kug, J.-S., Jeong, J.-H., Jang, Y.-S., Kim, B.-M., Folland, C. K., Min, S.-K., et al. (2015). Two distinct influences of Arctic warming on cold winters over North America and East Asia. *Nat. Geosci.* 8, 759–762. doi:10.1038/ngeo2517

Lehtonen, I., and Karpechko, A. Y. (2016). Observed and modeled tropospheric cold anomalies associated with sudden stratospheric warmings. *J. Geophys. Res. Atmos.* 121, 1591–1610. doi:10.1002/2015jd023860

Matthias, V., and Kretschmer, M. (2020). The influence of stratospheric wave reflection on North American cold spells. *Mon. Weather Rev.* 148, 1675–1690. doi:10.1175/mwr-d-19-0339.1

Maycock, A. C., and Hitchcock, P. (2015). Do split and displacement sudden stratospheric warmings have different annular mode signatures?. *Geophys. Res. Lett.* 42, 10943–10951. doi:10.1002/2015gl066754

Mitchell, D. M., Gray, L. J., Anstey, J., Baldwin, M. P., and Charlton-Perez, A. J. (2013). The influence of stratospheric vortex displacements and splits on surface climate. *J. Clim.* 26, 2668–2682. doi:10.1175/jcli-d-12-00030.1

Nakagawa, K. I., and Yamazaki, K. (2006). What kind of stratospheric sudden warming propagates to the troposphere?. *Geophys. Res. Lett.* 33, L04801. doi:10.1029/2005gl024784

Park, T.-W., Ho, C.-H., and Yang, S. (2011). Relationship between the Arctic oscillation and cold surges over East Asia. *J. Clim.* 24, 68–83. doi:10.1175/2010jcli3529.1

Rao, J., Garfinkel, C. I., and White, I. P. (2020). Predicting the downward and surface influence of the February 2018 and January 2019 sudden stratospheric warming events in subseasonal to seasonal (S2S) models. *J. Geophys. Res.* 125, e2019JD031919. doi:10.1029/2019jd031919

Renwick, J. A., and Wallace, J. M. (1996). Relationships between North Pacific wintertime blocking, El Niño, and the PNA pattern. *Mon. Weather Rev.* 124, 2071–2076. doi:10.1175/1520-0493(1996)124<2071:rbnpwb>2.0.co;2

Sung, M.-K., Jang, H.-Y., Kim, B.-M., Yeh, S.-W., Choi, Y.-S., and Yoo, C. (2019). Tropical influence on the North Pacific oscillation drives winter extremes in North America. *Nat. Clim. Change* 9 (5), 413–418. doi:10.1038/s41558-019-0461-5

Sung, M.-K., Kim, B.-M., Baek, E.-H., Lim, Y.-K., and Kim, S.-J. (2016). Arctic-North Pacific coupled impacts on the late autumn cold in North America. *Environ. Res. Lett.* 11, 084016. doi:10.1088/1748-9326/11/8/084016

Takaya, K., and Nakamura, H. (2001). A formulation of a phase-independent wave-activity flux for stationary and migratory quasigeostrophic eddies on a zonally varying basic flow. *J. Atmos. Sci.* 58, 608–627. doi:10.1175/1520-0469(2001)058<0608:afoapi>2.0.co;2

White, I., Garfinkel, C. I., Gerber, E. P., Jucker, M., Aquila, V., and Oman, L. D. (2019). The downward influence of sudden stratospheric warmings: association with tropospheric precursors. *J. Clim.* 32 (1), 85–108. doi:10.1175/jcli-d-18-0053.1

Conflict of Interest: The authors declare that the research was conducted in the absence of any commercial or financial relationships that could be construed as a potential conflict of interest.